Rheologic feedbacks between crystal preferred orientation and mantle flow driven by plate spreading

Donna Blackman[1], Olivier Castelnau[2], Donald Boyce[3], Paul Dawson[3], Gabi Laske[1]

[1]Scripps Institution of Oceanography, [2]Lab Procédés et Ingénierie en Mécanique et Matériaux, ParisTech, [3]Sibley school of Mechanical & Aerospace Engineering, Cornell University

Summary

Linked micro-macro scale numerical experiments explore the rheologic effects of crystal preferred orientation (CPO) and the magnitude of feedback on the pattern of upper mantle flow beneath slowly-spreading plates. The CPO and associated anisotropic rheology are coupled with a regional mantle flow model via a local viscosity tensor, which quantifies the stress:strain-rate response of a textured polycrystal. The olivine polycrystals have anisotropic viscosity for a significant portion of the model and this alters the flow, particularly near the base of the lithosphere. For background asthenosphere viscosity of 10^{20} Pa-s and a rigid lithosphere, the modification of the corner flow pattern is not drastic but the change could affect melting. Stronger fabric is predicted below the rift flanks for fully coupled, power law polycrystals than was determined using prior linear, intermediate coupling models. *SKS* splitting is predicted to be modestly different between intermediate and fully coupled cases for plates less than 20 Myr old. Surface waves, however, are predicted to have twice the magnitude of Rayleigh wave azimuthal anisotropy.

Model Resolution & Numerical Stability

Model discretization is specified separately for 4 regions, with finer node spacing within the (sub)axial and lithospheric regions. This is important for numerical stability in high flow gradient regions. In the models shown here we specify a stepwise increase in rigidity as temperature drops below 1000°C. Tests using more gradual viscosity transition across the base of the lithosphere show improved numerical stability in a narrow sub-plate zone. The figure below illustrates node spacing effects on the smoothness of the predicted velocity gradient. Numerical 'jitter' occurs as streamlines in the axial zone approach their 'freezing in' point (crossing the 1000° isotherm). This can impact details of predicted CPO within the lithosphere. We have determined that finer discretization will sufficiently address this but at this stage we retain the lower resolution model (B-1) in our assessment of the scale of the CPO-flow feedback.

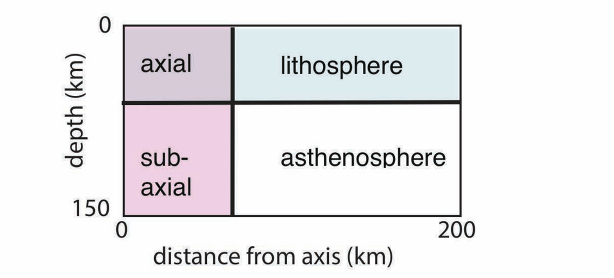

Finite Element size in subregions of the model & impact on local flow velocity (gradients). Flow gradient determines rate of crystal deformation.

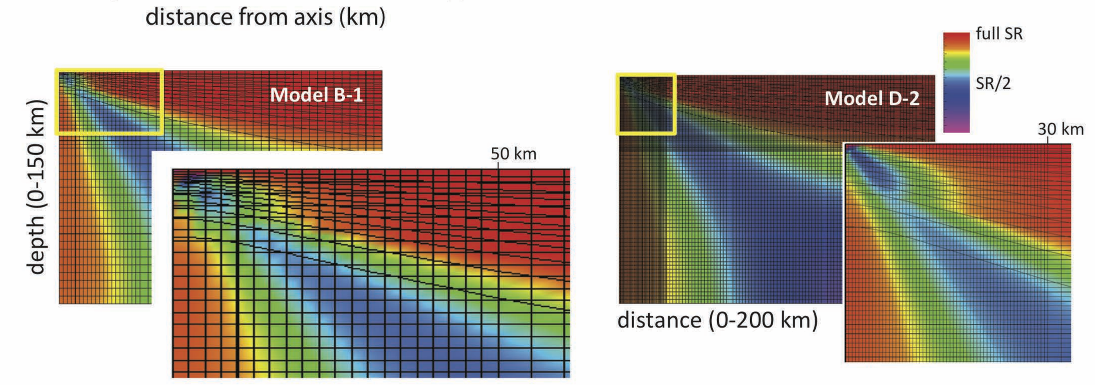

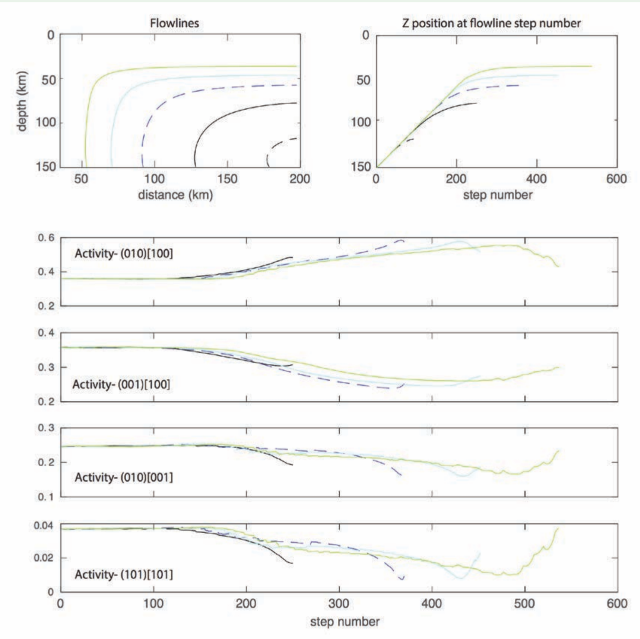

Activity of the specified olivine slip systems for polycrystals that travel along 4 example flowlines within the asthenosphere. The 4th, false system has critical resolved stress 2 orders of magnitude greater than the 3 main systems- it allows general deformation to occur without notably impacting the predicted CPO.

Slip along the *a-axis* dominates, as determined experimentally and in natural samples in dislocation glide regime for these pressure (P), temperature (T), and dry olivine conditions. Glide within the *b* plane overtakes that within the *c* plane as polycrystals turn the corner. Glide along the *b-axis* decreases away from the subaxial zone. Up to a few percent of the grains accommodate deformation via slip along the 4th, hard system.

For this exploration, we ignore other known deformation mechanisms. The scale of the viscosity anisotropy is based on predicted CPO which does still mimic that observed in natural mantle samples, so we are confident that our basic assessment is useful.

Basics & Modeling Approach

Olivine makes up ~70% of the upper mantle & single crystals have strongly anisotropic seismic propagation. A dominant mechanism to accommodate viscous flow stresses is slip along crystallographic planes via dislocation glide. Using linked finite element programs, we couple calculations of regional mantle flow and temperature with individual grain deformations within a polycrystal, which is subject to local flow field stresses. The initially random CPO of each polycrystal evolves constantly as it transits along a flowline, with the most favorably oriented slip system for each grain determining its latest deformation (new orientation).

Incorporation of the effect that local CPO has on viscosity is the important new step here. Moderate-strong CPO leads to anisotropic rheology and this can feedback on the flow pattern. At each flow-CPO iteration, we compute effective viscosity tensor for each local polycrystal- thus viscosity varies throughout the model and has directional dependence. The updated viscosity tensor is employed in the next flow iteration.

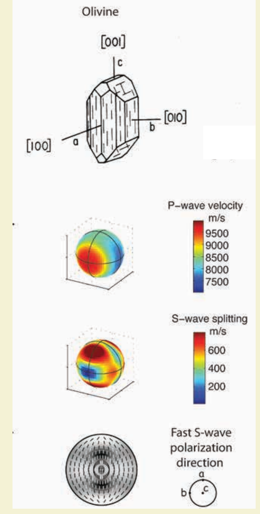

Single crystal olivine seismic anisotropy

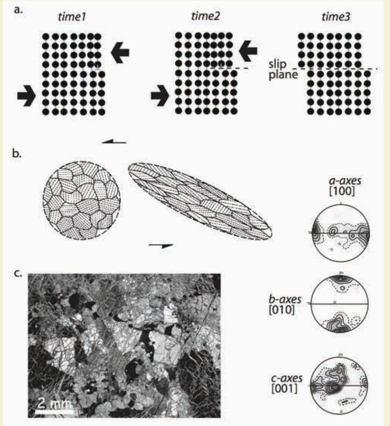

Illustration of disclocation glide: single crystal (top); polycrystal under shear (middle); CPO observed in mantle rock from Oman(lower, *Michibayashi et al., 2000*), with pole figures (right) showing concentrations of orientation for each of the 3 crystal axes.

Model Setup

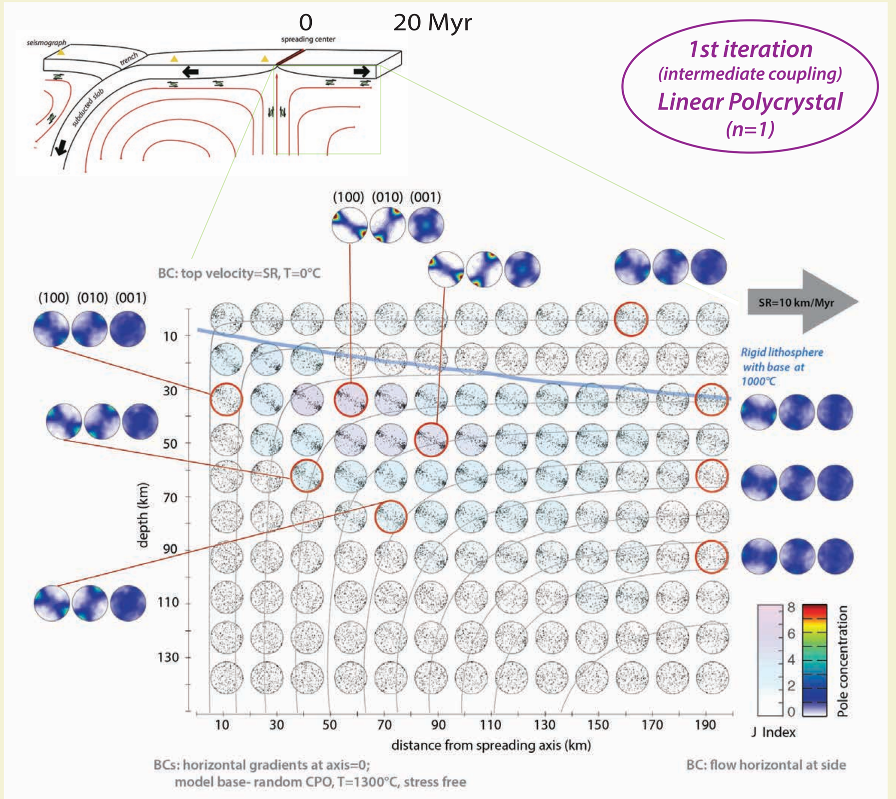

Reference slow-spreading model with constant, scalar asthenosphere viscosity (10^{20} Pa-s) & linear polycrystal. Asthenosphere 'corner flow' is driven by motion of rigid lithosphere (10^{23} Pa-s) , polycrystal paths from model base are shown by gray flowlines. Pole figures throughout model show *a-axis* orientation distribution (CPO) of 1000 olivine grains within local polycrystal. Contoured pole concentrations for all 3 crystal axes are shown at select locations. J-index color shading indicates CPO strength.

Initial Numerical Runs- Testing Stability, Effects of Polycrystal Stress:Strain-Rate Assumption

Prior attempts to integrate CPO-based viscosity tensor into regional flow predictions suggested that numerical instability could be a problem. Therefore, we first tested our linked flow-CPO-viscosity calculation for a simplified polycrystal. While individual grain slip system activity had usual nonlinear stress:strain-rate response, the aggregate of grains was specified to have linear behavior (stress exponent n=1). This allowed faster self-consistent solution times (hours to few-day) while indicating how the system evolved through many iterations. Flow & CPO stabilized after 15 iterations for this fully-coupled, linear polycrystal case.

Overall flow pattern is similar (gray streamlines, below), but subaxial upwelling rates are somewhat reduced compared to the reference case (1st iteration with isotopic viscosity and CPO accrued along reference streamlines, which is typical of what most previously publications predict) as shown at right.

Flow Velocity Difference: it15 - it1(=reference)

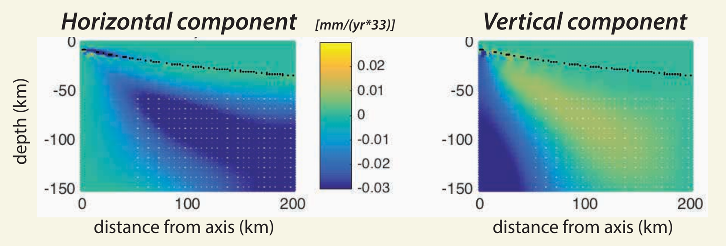

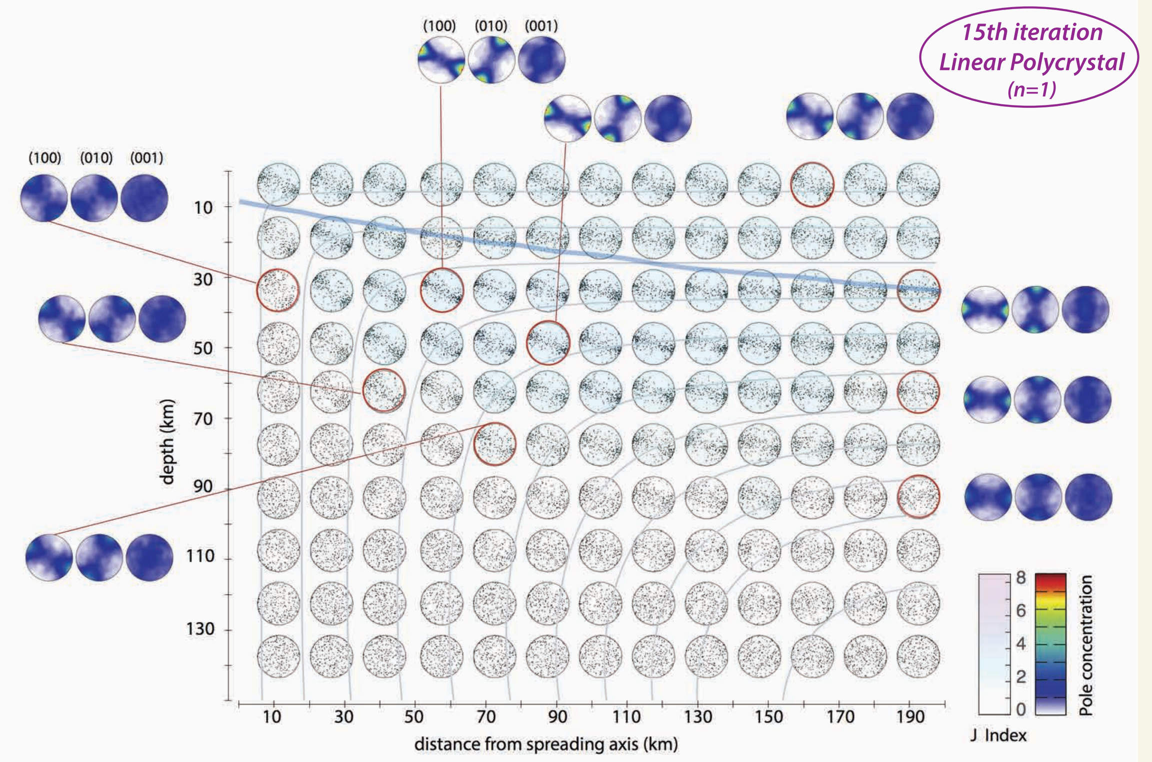

Figure format and color scales are the same as for reference model

Viscosity Tensor Components. Visualizing the viscosity tensor throughout the model space is challenging. At right, we show variation of the 6 independent components of the 6x6 tensor. Left panels are for the reference model (iteration 1), right panels are for iteration 15. Initially strong variation in the near-axis 'corner' of the flow is muted with evolution, as the CPO and flow pattern stabilize to self-consistent solution. Off-axis extent of the region that deviates significantly from isotropic value (green shade) grows.

The strength of the CPO is correspondingly reduced (J-index, at left) near the corner, but the thickness of the sub-plate aligned zone is greater and *a-axis* concentration changes from slightly inclined to horizontal at the edge of the model (20 Myr old plate).

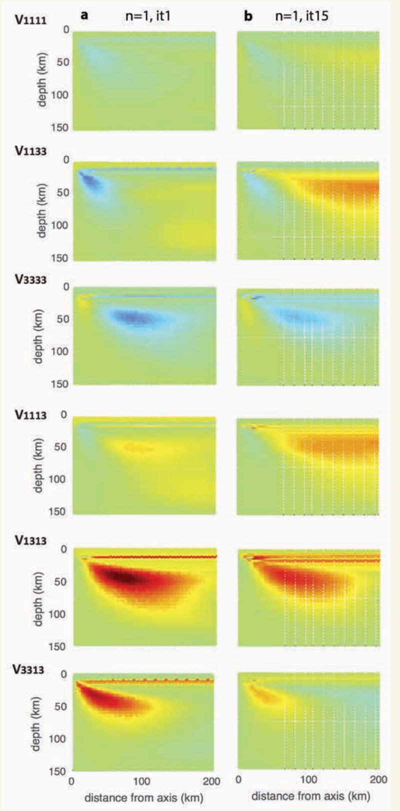

Power Law Polycrystal Effects

Polycrystal deformation is complicated due to grain-grain interactions; the exact stress:strain-rate relation is unclear. The homegenization scheme that we employ (*Castelnau et al., 2009*) approximates average effects of surroundings on a given grain for a specified polycrystal stress exponent *n*. Experiments to date suggest that a stress exponent of ~n=3 may be appropriate. For both numerical stability and computation cost reasons, we take a stepwise approach toward more realisitic model: we test power law polycrystal cases with *n=2* and *n=3* , compare outcomes, and assess how well simpler models capture the essence of the results. By using the Second-Order Visco-Plastic Self Consistent (VPSC-SO) formulation, we are able to address rheologic behaviors where standard VPSC breaks down (*Ponte-Castenada, 2002*).

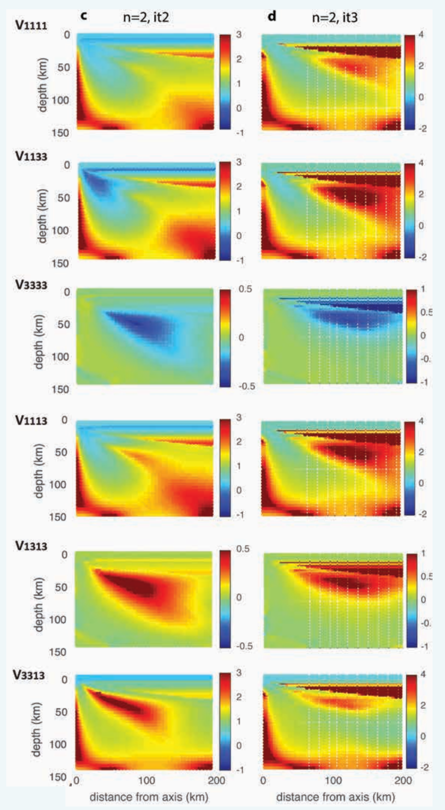

Viscosity Tensor Components.
As expected, viscosity tensor deviates from isotropic more strongly for power law polycrystal than for the linear case (color scale is same as for it1:it15 comparison, with pale green indicating essentially isotropic value in a region of the model). As for the linear case, the initially strong signal for the near-axis corner of the flow is reduced over subsequent iterations and the strength and extent of the signal beneath the off-axis lithosphere increases with iteration.

While we have not continued to a fully stablized self consistent flow-CPO-viscosity model yet, our early iterations do capture the scale of the feedback effect, which was the main goal of this phase of the study.

The similarity in predicted seismic anisotropy (below) for the *n=2* and *n=3* linear polycrystal cases, suggests that the former may capture main aspects of signal for power law cases. We pursue *n=2* behavior at this stage because it is significantly less computationally intensive. Future work will test *n=3* iteration explicitly.

Seismic Anisotropy. Elastic constants associated with each textured polycrystal are computed by Voigt-Reuss-Hill average of single crystal properties projected into the model frame. In addition to showing SKS splitting (top panels) that would be measured at the surface (or seafloor for oceanic spreading), we show local P-wave anisotropy (2nd row), & local splitting for waves inciden ±20° from vertical (3rd and 4th rows).

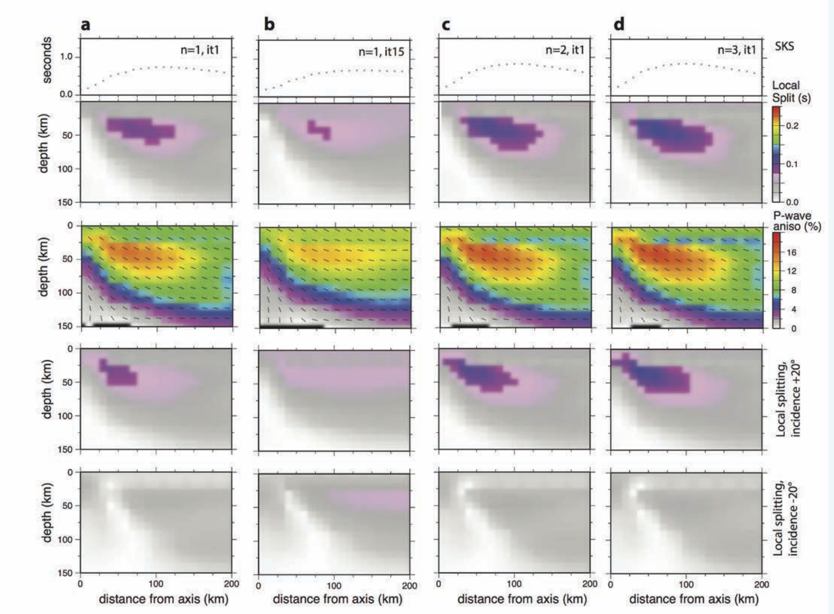

Fully Coupled, Power Law Polycrystal Case

The flow pattern, CPO, and viscosity distribution for *n=2* case does not oscillate between the 1st and 3rd iteration, there is a steady, positive feedback between the anisotropic, CPO-based viscosity and evolution in the flow field. While our *n=2, it3* solution is not a final self-consistent solution, we can be confident that our current prediction is a conservative estimate of the scale of the feedback and magnitudes of associated seismic anisotropy.

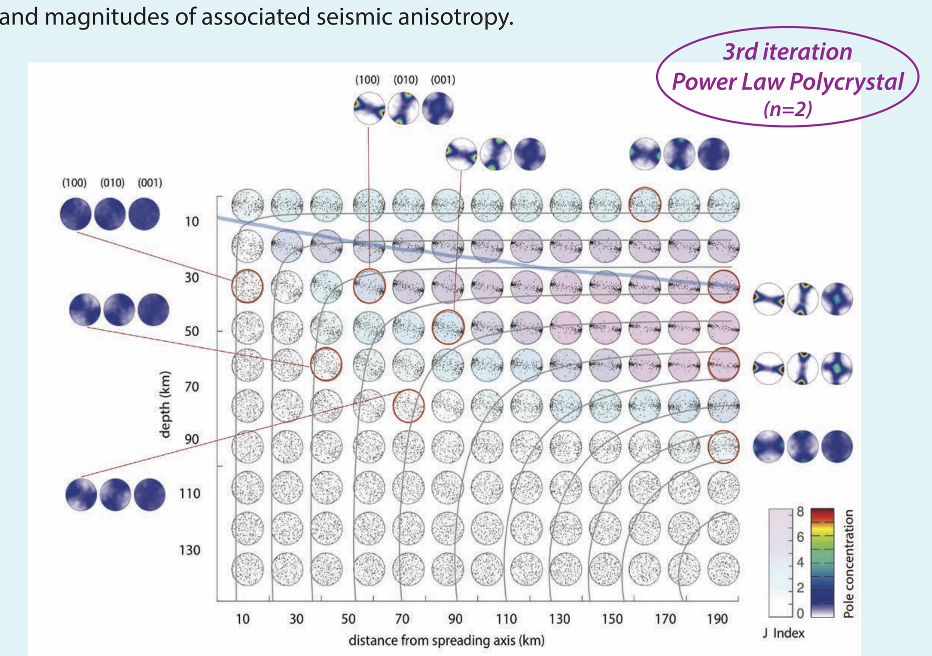

Figure format and color scales are the same as for reference model

Again, changes in the overall flow pattern are modest, but the predicted CPO near, and below, the off-axis lithosphere base is notably stronger than for the reference case. *b-axis* concentrations are subvertical and *c-axis* concentrations have point maxima, rather than girdles, beneath the 20 Myr old plate. Alignment within the lithosphere is stronger.

Body Wave Anisotropy

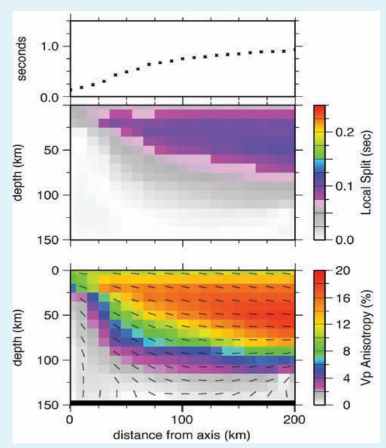

Rayleigh Wave Sensitivity & Anisotropy

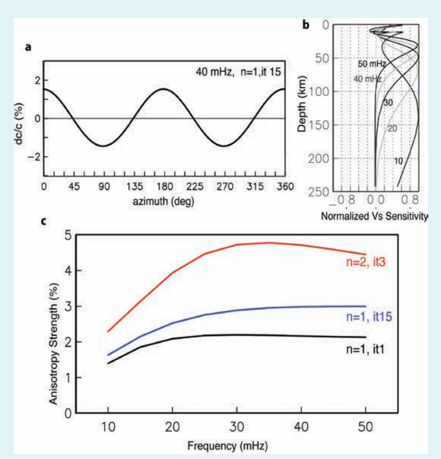

SKS splitting predicted at the surface (seafloor) differs only modestly from the reference case (left top), although P-wave travel-time signature would be more discernible between the cases due to greater relative delay from the axis out to 15-20 Myr old lithosphere (left, lower). Rayleigh wave anisotropy is predicted to be about twice as great at the oldest part of the model as in the reference case (right, lower).

Highlights & Next Steps

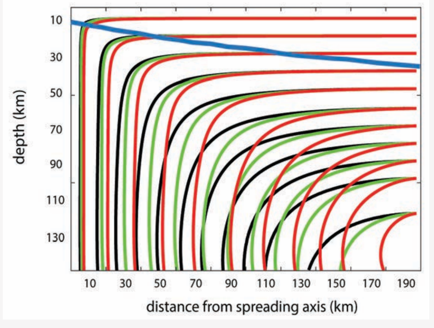

Comparison of flow pattern. isotropic viscosity case (black *it1*); fully coupled, self consistent linear polycrystal case (green *n=1, it15*); fully coupled power law polycrystal case (red *n=2, it3*).

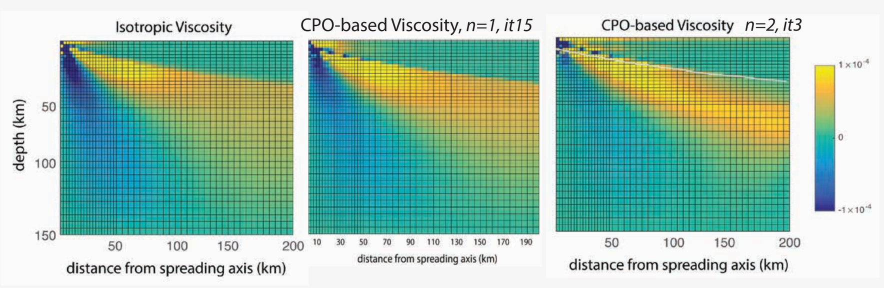

Comparison of Strain Rate Within the Model. High strain-rate region thickens with age off axis as CPO enhances deformation subparallel to the direction of plate motion within a band below the lithosphere. This effect is stronger for power law polycrystal than linear, as expected.

- *further n=2 iteration til fully self consistent*
- *test additional n=3 flowlines, to assess difference from n=2*
- *case with background viscosity 10^{18} Pa-s, more appropriate for spreading center*
- *upgrade model so only partial flowline backtracking is required; will greatly reduce computation time*
- *compute lateral variations in surface wave predictions*

References on this method of flow/CPO/viscosity calculation

Blackman, D.K., H-R. Wenk & Kendall, J.-M., 2002. Seismic anisotropy in the upper mantle: 1. Factors that affect mineral texture and effective elastic properties, G-Cubed, doi 10.1029/2001GC000248

Blackman, D.K. and J-M. Kendall, Seismic anisotropy in the upper mantle: 2. Predictions for current plate boundary flow models, G-Cubed 10.1029/2001GC000247, 2002.

Blackman, D.K., D.E. Boyce, O. Castelnau, P. R. Dawson, and G. Laske, Effects of crystal preferred orientation on upper mantle flow near plate boundaries: Rheologic feedbacks and seismic anisotropy, Geophysical J. Intl., in revision 2017.

Castelnau, O., D. K. Blackman & Becker, T.W., 2009. Numerical simulations of texture development and associated rheological anisotropy in regions of complex mantle flow, GRL, 36, doi:10.1029/2009GL038027.

Castelnau, O., D. K. Blackman, R. A. Lebensohn & Castañeda, P.P., 2008. Micromechanical modeling of the viscoplastic behavior of olivine, J. Geophys Res., 113 doi:10.1029/2007JB005444.

Cho, J.-H., D.E. Boyce & Dawson, P.R., 2007. Modelling of strain hardening during friction stir welding of stainless steel, Modelling Simul. Mater. Sci. Eng., 15, 469-486 doi:10.1088/0965-0393/15/5/007.

Cho, J.-H. & Dawson, P.R., 2008. Modeling Texture Evolution During Friction Stir Welding of Stainless Steel With Comparison to Experiments, J. Eng. Mat. Tech., 130 DOI: 10.1115/1.2816902.

Dawson, P. & Wenk, H., 2000. Texturing of the upper mantle during convection, , Phil. Mag. A, 80, 573-598

Lebensohn R.A., P. Ponte Castañeda, R. Brenner, O. Castelnau, Full-field vs. Homogenization methods to predict microstructure-property relations for polycrystalline materials, Computational Methods for Microstructure-Property Relationships, Chap. 11, p.393-442, Ed. S. Ghosh and D. Dimiduk, Springer, 2011

Ponte Castañeda, P., 2002. Second-order homogenization estimates for nonlinear composites incorporating field fluctuations. I. Theory, J. Mech. Phys. Solids, 50, 737–757

Raterron, P., F. Detrez, O. Castelnau, C. Bollinger, P. Cordier, S. Merkel, Multi-scale modeling of upper mantle plasticity: from single-crystal rheology to multiphase aggregate deformation, PEPI 228, 232-243, doi: 1016/j.pepi.2013.11.012, 2014.